EUROPEAN ORGANIZATION FOR NUCLEAR RESEARCH

CERN-AT-95-19

CERN AT/95-19 (MA)
LHC Note 328

Finite Element Structural Analysis of LHC Bending Magnet

R. Perin, D. Perini, J. Salminen, J. Soini*

FE-calculations have been carried out for the cross-section of the 56 mm superconducting LHC dipole prototype with aluminium common collar and a vertically split yoke. The structure has been studied at room temperature and at 1.8 K both energized and non-energized. Collaring and assembly procedure were also modelled. Considerations are also made about the influence of the tolerances on the behaviour of the structure.

*Picker Nordstar Oy, Helsinki, Finland

Magnet Technology Conference (MT14), 11-16 June 1995, Tampere, Finland

Geneva, Switzerland
9 November 1995

Finite Element Structural Analysis of LHC Bending Magnet

Romeo Perin, Diego Perini, Jukka Salminen
CERN, 1211 Geneva 23, Switzerland

Jouko Soini
Picker Nordstar Oy, Helsinki, Finland

Abstract **FE-calculations have been carried out for the cross-section of the 56 mm superconducting LHC dipole prototype with aluminium common collar and a vertically split yoke. The structure has been studied at room temperature and at 1.8 K both energized and non-energized. Collaring and assembly procedure were also modeled. Considerations are also made about the influence of the tolerances on the behaviour of the structure.**

I. Introduction

A number of model and prototype dipoles of different lengths (1 m, 10 m, 15 m) for the LHC will be built in the near future. These magnets will have a coil aperture diameter of 56 mm and a new cross-section (Fig. 1).
The aim of the present analysis and optimization was to define the nominal dimensions so that favorable stresses can be obtained under all load cases. Compressive stresses must be present anywhere in the coils in all working conditions. Everywhere in this paper we call "gap size" the difference between the nominal size of the adjacent pieces in undeformed conditions.

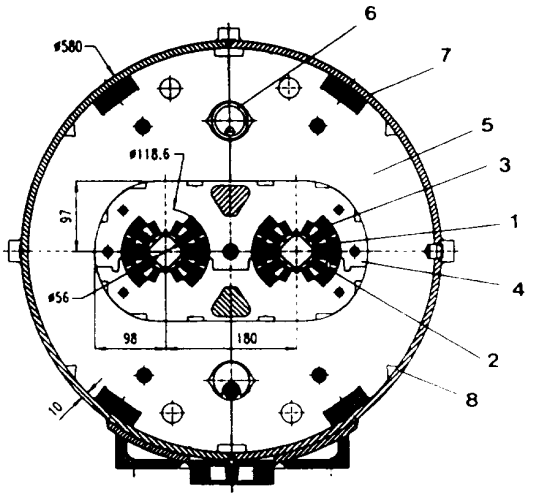

Fig. 1. Cross-section of LHC dipole magnet. 1. Beam-screen, 2. Beam pipe, 3. Superconducting coils, 4. Non-magnetic collars, 5. Iron yoke, 6. Heat exchange tube, 7. SC bus-bars, 8. Shrinking cylinder / He II-vessel

Manuscript received June 13, 1995. Jukka Salminen, e-mail salminen@parcb.cern.ch, phone +41-22-767 3291, fax +41-22-767 6300: Diego Perini, e-mail perinid@cernvm.cern.ch

II. Finite-Element Model

A central field of 9.7 T was assumed for the mechanical design of the structure, which was studied by means of the ANSYS[1] finite element package. The electro-magnetic forces at 9.7 T have been computed taking into account iron saturation. From this the same finite element package calculated the stresses and strains present in the structure. No friction has been considered.
A two dimensional model has been meshed and the plane stress option has been used in the elements. Through the magnet's longitudinal section, every second collar only is keeping the forces that are exerted by the coils. It was possible to simulate such a structure by creating two layers of 0.5 mm thick mesh for the collars. For the coils, iron yoke, cylinder and pins a one 1mm thick layer is meshed.
The areas have been meshed using two dimensional linear type 42 [4] elements and contact surfaces with three dimensional type 52-contac [4] elements. Further information concerning these elements are available from the ANSYS-manuals.
The prestress of the coils is imposed by giving an interference at the interfaces between the collars and the coil heads. The external cylinder prestress is also simulated by giving an interference at the interface between the iron yoke and cylinder.
The geometry is modeled at room temperature and in non-deformed conditions. That is to say the dimensions used in the model are for parts in their nominal size, as produced.

III. Collaring

A. General

During the collaring, the collars are assembled with a given interference around the coils. The compression of the coils reaches the maximum value under the press just before the insertion of the pins. Once the pins are in, and the pressure is released, part of the compression is lost, because of the deformation of the collars.
In order to limit the stresses in the coils under the press, it is necessary to elongate the collar legs during the collaring process. This is obtained by pushing on the slots in the col-

[1] ANSYS is trademark of Swanson Analysis Inc.

lars. If for the sake of simplicity all non-linear phenomena are ignored the coil-collar structure of a single aperture can be simulated using springs (Fig. 2).

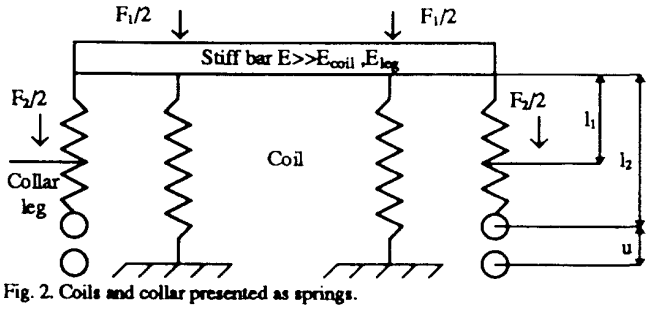

Fig. 2. Coils and collar presented as springs.

If the collaring force is applied at the top of the collars, the coils have to deform by length u, to allow the insertion of the locking rods. If the spring constant of the coil is marked with k_{coil}, the force needed to insert the rods is therefore:

$$F1 = 2 \cdot u \cdot kcoil \qquad (1)$$

If the collaring force is applied only on the side of the collars the force that is needed will be:

$$F2 = \frac{2 \cdot u \cdot kcoil}{1 + \frac{kcoil}{kcollar}} \qquad (2)$$

Where k_{collar} is the spring coefficient of the collar legs. Since the central post of the collar is much stiffer than the legs, most of the spring back effect is the result of the leg elastic deformation of the local deformation around the pins. When the press is released and the locking pins are placed, the compression force in the coil is taken by the length 'l_2'. Therefore relaxation of the stress in the coil is smaller if we press close to the horizontal axis. However, it is not possible to push only at the extreme edges of the collars, since stresses might become excessive due to the fact that there is not enough surface area to apply the forces. Therefore it is necessary to apply part of the collaring force at the top of the collars.

We can define a relaxation ratio as a ratio between the vertical forces on the horizontal median plane of the coils after (Fyls2) and before (Fyls1) the press is released.

$$\frac{F_{yls2}}{F_{yls1}} = \frac{1313.6 + 1139.3}{2541.5 + 2658.3} \times 100 \approx 47.2\% \qquad (3)$$

From Table I it can be seen that the relaxation ratio of the central side (nearer to the magnet central axis) coil is lower than that for the lateral side. This is due to the fact that there is higher stress concentration near the central key pin and consequently higher deformation at this point. To show the advantage of pre-pulling the collar legs, we have calculated a case where only the top of the collar is pressed. This is shown in the Table I. The relaxation is:

$$\frac{F_{yls2}}{F_{yls1}} = \frac{1271.8 + 1145.3}{2626.7 + 3001.1} \times 100 \approx 42.9\% \qquad (4)$$

This means that the relaxation can be reduced by 4.3% by elongating the collar legs during the collaring process.

TABLE I
STUDY OF THE COLLARING PROCESS

	Preferred procedure		Pressure on collar top only	
	Under press	Press released	Under press	Press released
Forces [N/mm/½ collar][a]				
At top of the tool	-5199.8	–	-5627.8	–
Coil right(hor plane)	2541.5	1313.6	2626.7	1271.8
Coil left (hor plane)	2658.3	1139.3	3001.1	1145.3
Total Fy	5199.8	2452.9	5627.8	2417.1
Coil stresses along the coil mid plane [MPa]				
σaverage	84.4	39.8	91.4	39.2
σ inner coil right	85.8	41.6	86.8	40.3
σ inner coil left	90.5	37.4	104.5	37.3
σ outer coil right	79.2	43.7	83.8	42.3
σ outer coil left	82.1	36.6	90.4	37.1
Vert. offset of locking rod center from hor. axis [mm]				
Right	-1.1×10^{-3}	–	-0.0125	–
Left	-7.3×10^{-3}	–	-3.8×10^{-3}	–

[a] All forces are for one coil (half a collar) per mm.

IV. ASSEMBLY OF THE MAGNET

The maximum vertical displacement (0.268mm) in the collared coil pack occurs at the vertical symmetry plane above the iron insert (Fig. 3). Elsewhere the displacements at the top of the fixed collars are 0.14-0.18mm. To avoid the need for special tooling the shape of the iron yoke takes into account the deformed shape of the collars after collaring.

It is possible to open the 'C' shaped half-yoke by a maximum of about 0.2 mm from the symmetry plane before the azimuthal tensile stresses near the horizontal plane become excessive (i.e. 0.23 mm vertical displacement of the point x0 gives rise to 100 MPa tensile stress at the point E Fig. 3). The gap size between x0-x38 is 0.2 mm (Fig. 3). In this way the collar assembly can be placed into the yoke, only in the final stages of the assembly a small interference of 0.07 mm between yoke and the collar appears.

V. COMPLETE MAGNET

A. General

To avoid any conductor movement under the influence of the electro-magnetic forces the conductors should be well supported when the magnet is energized. During excitation the e.m. forces will unload the pressure between the central post and the first turn of the coil. When the magnet is at maximum field some azimuthal compression is still needed to ensure that no cracks or sudden displacements occur in the coils. On the other hand to avoid the deterioration of the coil

through creep, the room temperature prestress should not be too high [5].

During cool down from room temperature to 1.8 K the iron contracts much less than the collars. To compensate for the different contractions, there is a vertical gap in the iron. This gap permits the iron to follow the collars contraction. A good contact between collars and iron yoke as well as a strong mating force between the iron yoke halves can warrant a rigid structure.

B. Discussion of the Results

The assembled magnet has been analyzed at room temperature, at 1.8 K, Bo = 0 T and at 1.8 K, Bo = 9.7 T.

The parameters, stresses and displacements of the structure in the considered different load steps are reported in the Tables II-V and Fig. 3.

TABLE II

OPTIMIZED PARAMETERS OF THE MECHANICAL DESIGN

Vertical gap size/half gap		
at the top (D_o)	0.62	mm
at the bottom (D_I)	0.47	mm
Collar-yoke gap size		
bottom at 0°	0	mm
at 25°	0.04	mm
at 38°	0.3	mm
x=59	0.3	mm
x=38	0.2	mm
x=0	0.2	mm
Interference between collars and coils		
inner coil r=28	0.28	mm
inner coil r=45.2	0.3	mm
outer coil r=45.7	0.3	mm
outer coil r=62.9	0.33	mm
Collar nose slot		
width/height	4x3.8	mm
Yoke-shrinking cylinder		
radius interference	-0.43	mm

TABLE III

DISPLACEMENTS IN SOME SIGNIFICANT POINTS

Load Step	293K	0T	1.8K	0T	1.8K	9.7T
Points	U_x	U_y	U_x	U_y	U_x	U_Y
A	-0.199	0	-1.04	0	-0.995	0
B	0	-0.079	0	-0.793	0	-0.823
D	-0.276	-0.073	-0.620	-0.725	-0.620	-0.756
D_I	-0.237	-0.052	-0.47	-0.380	-0.470	-0.404
E	-0.189	0	-0.819	0	-0 768	0
K_{right}	-0.190	0	-0.531	0	-0.444	0
K_{left}	0.002	0	-0.250	0	-0.282	0
MU^a	-0.037	0.236	-0.413	-0.201	-0.408	-0.252
MF^a	-0.035	0.227	-0.413	-0.212	-0.408	-0.262

[a]Collars are divided into two layers: fixed (Mu*) and floating (Mf*)

TABLE IV

AZIMUTHAL STRESSES IN SOME SIGNIFICANT POINTS OF THE COILS

Point	293K 0T	1.8K 0T	1.8K 9.7T	
1	-71	-70	-94	MPa
2	-81	-77	-42	MPa
3	-60	-61	-98	MPa
4	-62	-58	-24	MPa

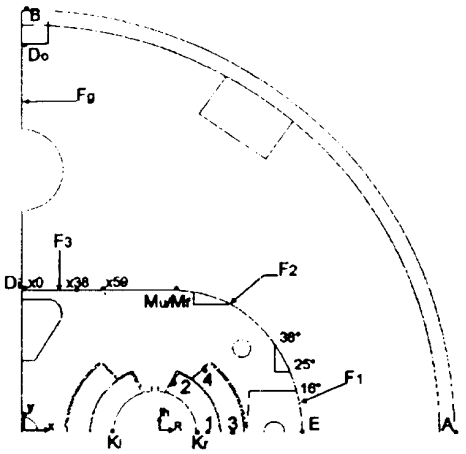

Fig. 3. Parameters for the mechanical optimization and significant points.

TABLE V

CHARACTERISTIC DATA OF THE MECHANICAL DESIGN

Load step	293K 0T	1.8K 0T	1.8K 9.7T	
Vertical gap				
Fg	0	1738	713	N/mm
Size at top	0.34	0	0	mm
Size at bottom	0.23	0	0	mm
Collar-yoke interface				
F1(0°-25°)	1673	552	1626	N/mm
F2(38°≤x≤59)	0	0	0	N/mm
F3(0≤x≤38)	1044	513	658	N/mm
Max. shrinking cylinder stress on horiz plane	156	230	226	MPa
Lorentz force in right coil quadr. (9.7T)				
Fx	0	0	2248	N/mm
Fy(out. layer)	0	0	-194	N/mm
Fy(inn. layer)	0	0	-823	N/mm

The nominal gap between yoke and collar quadrants increases as a function of the angle . The gap is zero at the horizontal plane (0°) and increases linearly to a size of 0.04 mm at 25°. A gap of 0.2 mm has been left from the point x38 to the point x59 in order to avoid contact during the assembly (Fig. 3).

The vertical iron yoke gap is open at room temperature and completely closed at 1.8K. When the magnet is energized the gap remains closed.

At room temperature a relatively strong contact exists between collars and yoke (Table V). At 1.8K the normal resulting force decreases due to the fact that the aluminium collars shrink more than the surrounding yoke. At 9.7T the collars have line to line fit from -5° to 25°.

During collaring the stress in the coils reaches its maximum value at room temperature. The compression is higher at the innermost corner of the top of the inner coil layer. Moreover the vertical gap is completely open at room temperature and all the horizontal forces coming from the shrinking cylinder are taken by the collars. Part of this force is then transmitted to the coils. This increases the azimuthal stresses at the innermost corner of the top of the inner coil layer. In order to reduce these stresses a 3.8 mm deep and 4 mm wide slot has been cut out in the middle of the collar post.

VI. TOLERANCES

The influences of manufacturing tolerances on mechanical behaviour of the magnet have been studied. To understand causalities and keep the number of the analysis reasonable, only one parameter per time has been changed.

The following parameters have been studied (Fig. 3):

- Gap size between collar and yoke at 25°
- Gap size between collar and yoke from 0° to 25°
- Gap size between collar and yoke from x0 to x38
- Half vertical gap size between yoke-halves from D_i to D_o

For small shifts around the nominal dimensions, we can get, for a certain force Fi:

$$F_i = F_{i0} + \sum \frac{\partial F_i}{\partial Gap_j} \cdot dGap_j \qquad (5)$$

where F_{i0} is the nominal force and every differential term can be evaluated as the "slope" of the curve representing the force i vs. the gap j shift. If the variations are small around nominal dimensions, forces behave linearly with tolerances. We can therefore define a matrix of the slopes [S]:

$$[F] = [S] \cdot [u] + [F_0] \qquad (6)$$

where [u] are the shifts [mm], [F] the forces [N/mm] due to these shifts and [Fo] the forces [N/mm] due to the nominal gap values. The influence of vertical gap, (0°-25°) gap and (x0-x38) gap shifts on the corresponding mating forces can be evaluated using the following matrix:

$$[S] = \begin{bmatrix} -10150 & 1675 & 6450 \\ 1525 & -6825 & -2525 \\ 6625 & -2500 & -7875 \end{bmatrix} \left[\frac{N}{mm^2}\right] \qquad (7)$$

and the complete equation:

$$\begin{bmatrix} F_{VertGap} \\ F_{(x0-x38)Gap} \\ F_{(0°-25°)Gap} \end{bmatrix} = \begin{bmatrix} -10150 & 1675 & 6450 \\ 1525 & -6825 & -2525 \\ 6625 & -2500 & -7875 \end{bmatrix} \cdot \begin{bmatrix} \Delta_{VertGap} \\ \Delta_{(x0-x38)Gap} \\ \Delta_{(0°-25°)Gap} \end{bmatrix} + \begin{bmatrix} 713 \\ 513 \\ 552 \end{bmatrix} \left[\frac{N}{mm}\right] \qquad (8)$$

In table VI two 'limit cases' are presented. In the first case the normal contact force F_1 between collars and yoke has been minimized by choosing all the tolerances in a unfavorable way. In the second case the vertical mating force F_g has been minimized. It is recalled that the nominal forces F_g, F_1 and F_3 are 713 N/mm, 552 N/mm and 513 N/mm respectively. Results have been compared with ANSYS to check the accuracy of the estimation. We can see reasonable correspondence, except for the force F_1 with very low values, where the simplified model is over pessimistic. This can be explained by the fact that the forces behave unlinearly with low force levels (Fig. 4). Due to the approximations of the model a reasonable safety margin has to be considered. This is the reason why far from the nominal conditions low forces are less interesting.

TABLE VI
RESULTING CONTACT FORCES WHEN ALL DIMENSIONAL TOLERANCES HAVE BEEN CHOSEN SUCH AS TO MINIMIZE F_1 AND F_g

	Shift [mm]	F_g [N/mm] (1.8K, 9.7T)	F_1 [N/mm] (1.8K)	F_3 [N/mm] (1.8K)
Nominal force [F_0]		713	552	513
Vertical gap	-0.04	+406	-265	-61
0°-25° gap	0.02	+129	-157.5	-50.5
x0-x38	0.03	+50.2	-75	-204.7
Total estimated matrix [F] (8)		1298.2	54.5	196.7
Total force by ANSYS		1294	112.5	219.9
Error		0.3 %	-51.5%	-10.5%
Nominal force [F_0]		713	552	513
Vertical gap (F_g)	0.04	-406	+265	+61
0°-25° gap (F_1)	-0.02	-129	+157.5	+50.5
x0-x38 (F_3)	-0.03	-50.2	+75	+204.7
Total estimated matrix [F] (8)		127.8	1049.5	829.2
Total force by ANSYS		145	1069	839
Error		-11.9 %	-1.8 %	-1.2 %

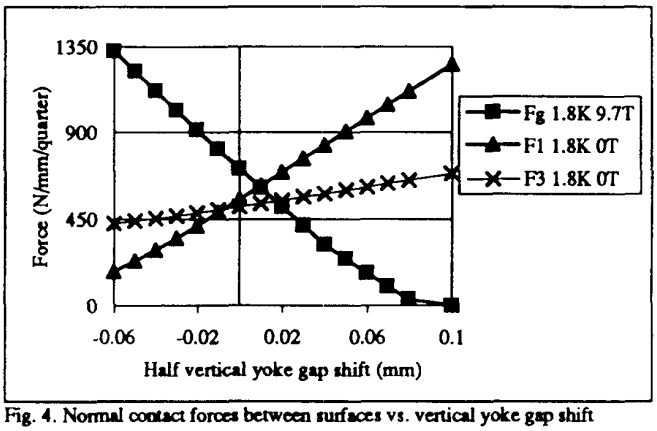

Fig. 4. Normal contact forces between surfaces vs. vertical yoke gap shift

REFERENCES

[1] The LHC Study Group, "LHC The Large Hadron Collider Accelator Project," Geneva 1993, CERN, CERN/AC/93-03(LHC).

[2] "Design features of the new LHC dipole long models (prototypes)," Edited by Perin, R. Geneva 1994, CERN, Internal Note 94-103

[3] Bona M., Perini D., "Finite element structural analysis of the twin aperture prototype superconducting magnet for the large hadron collider," Geneva 1990, CERN, LHC Note 120.

[4] "ANSYS User's Manual for Revision 5.0," Houston 1992, Swanson Analysis Systems Inc.

[5] Meß K. H., Schmüser P., "Superconducting Accelerator magnets, Superconductivity in particle accelerators," Geneva 1989, CAS CERN Accelerator school.

[6] Maffezzoli A., Perini D., Salminen J., Soini J. "Finite-element structural analysis of LHC bending magnet," Geneva 1995, CERN, Internal note 95-127.